Figure S1

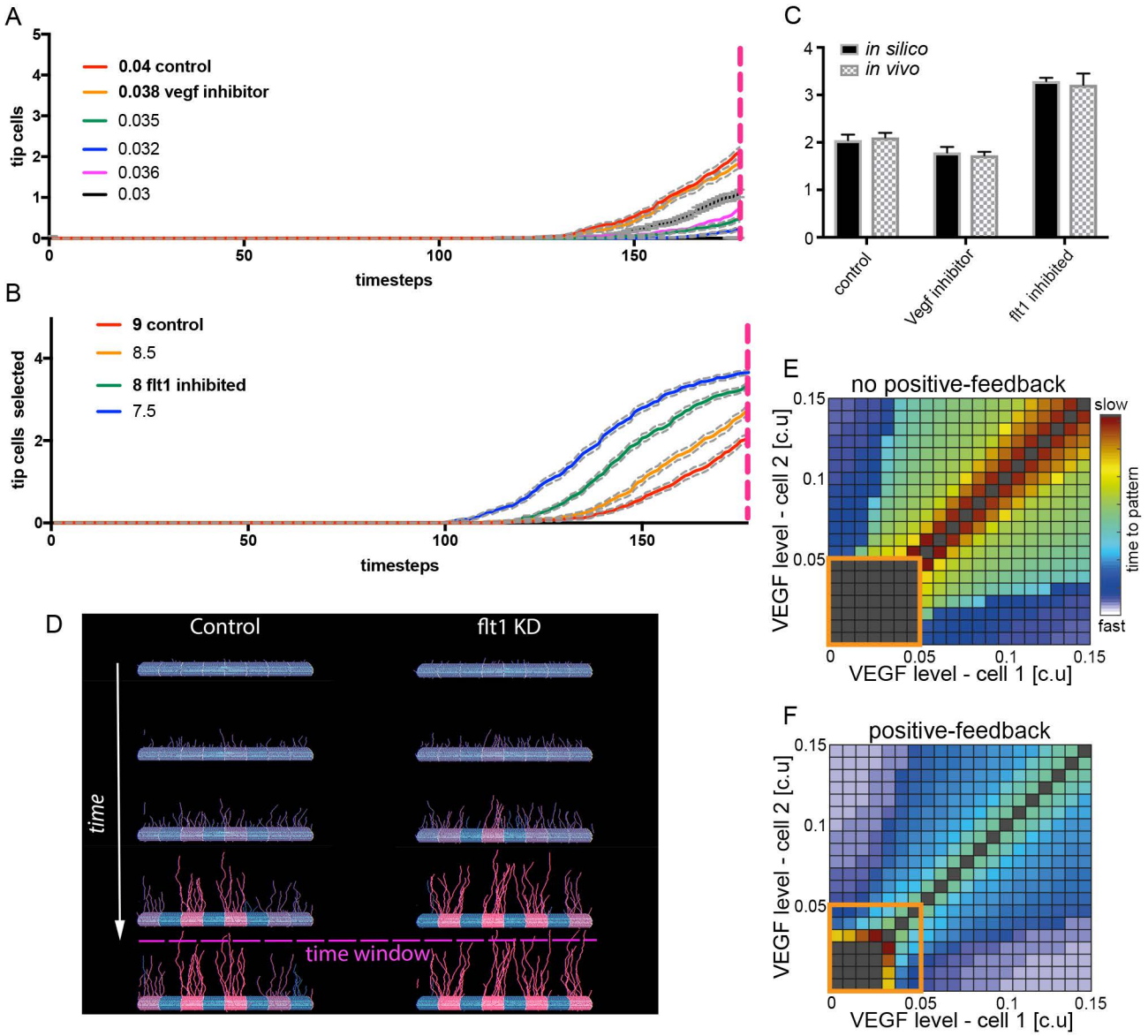

Figure S1. VEGFR signaling and positive-feedback define the magnitude and timing of tip EC selection *in vivo*, related to Figure 1. (A-B) MSM modeling of the influence of differential Vegfr (A) and flt1 (B) levels on the timing of EC activation via lateral inhibition. By defining a selection window at approximately 175-time steps, the model accurately recapitulates the *in-vivo* behavior induced by Vegfr inhibition (decreased EC selection) and *flt1* knockdown (increased EC selection) in Figure 1C. (C) Quantification of the number of cells selected in the selection window both *in silico* and *in-vivo.* (D) Example frames from one simulation run of a control simulation (Vsink=9) vs a flt1 KD simulation (Vsink =8) showing by the end of the time window the control is actually less efficient, i.e. slower to select within the time window as the flt1 KD selects all possible tip cells from the available pool of cells more rapidly. Frames taken at t=0,50,100,150,200. (E-F) Matrix plots of EC patterning speeds in the 2-cell ODE system following exposure of each cell to different VEGF levels in the absence (E) or presence (F) of positive-feedback. Grey boxes indicate either the failure to adequately pattern into Vegfr active and Notch active ECs or very slow patterning. Larger orange boxes indicate coupled ECs experiencing the lowest VEGF levels (<0.05 c.u.). Positive-feedback globally increases the speed of cell patterning and greatly reduces the threshold of VEGF levels capable of generating robust patterning (see large orange boxes).

Figure S2

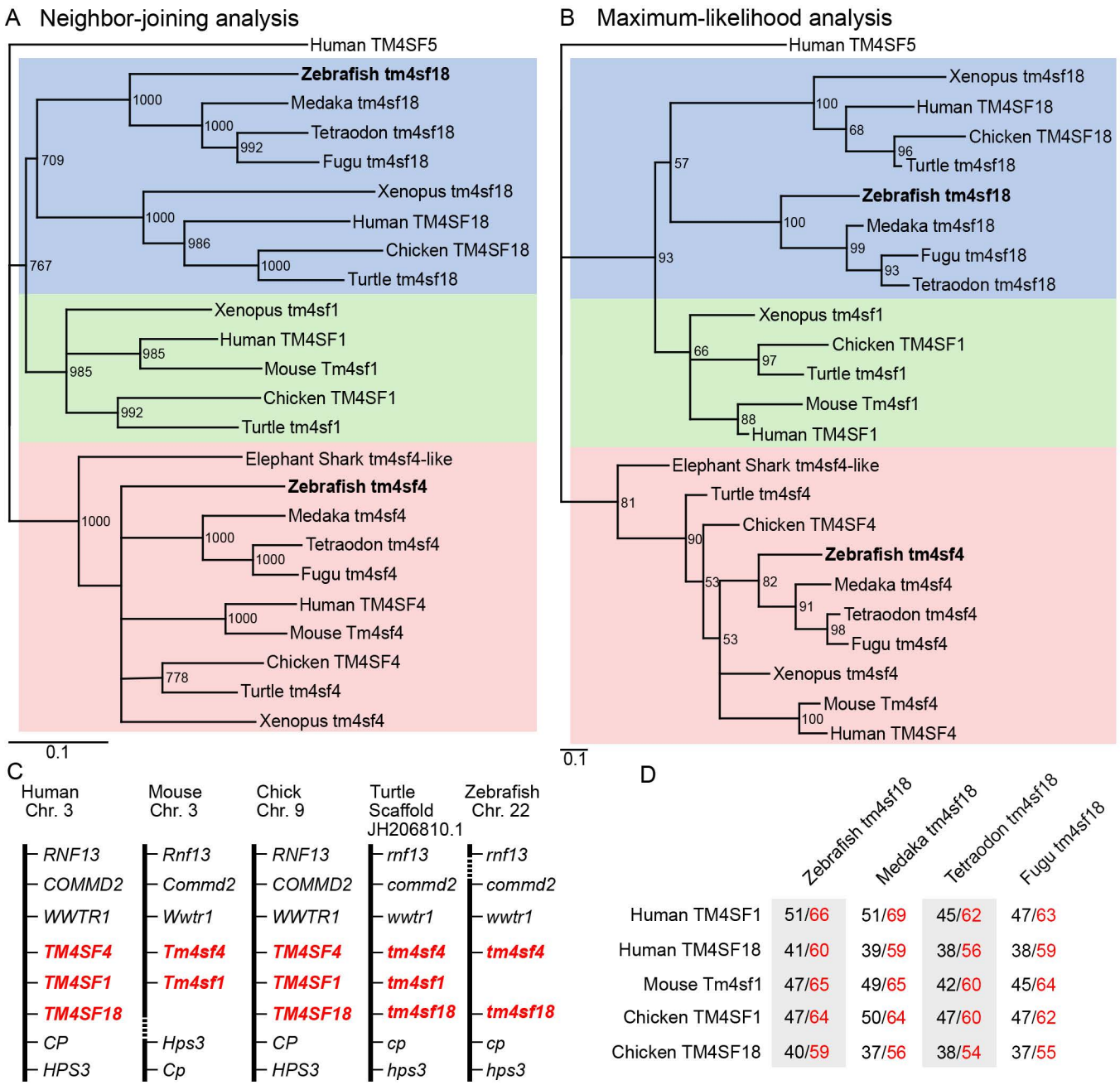

Figure S2. Phylogenetic, synteny and protein analysis of the TM4SF family, related to Figure 2. (A-B) Phylogenetic trees of vertebrate TM4SF1/4/18 protein family based on either neighbor-joining (NJ, A) or maximum-likelihood (ML, B) analyses. Human TM4SF5 protein sequence was defined as the out-group. Branch lengths are proportional to evolutionary distance corrected for multiple substitutions; the scale bar denotes 0.1 underlying amino acid substitutions per site. Figures on branches indicate robustness of each node (>50%), estimated from 1000 bootstrap replicates for NJ (A) and 100 replicates for ML (B). All nodes with a bootstrap support of less than 50% were collapsed to a polytomy. Based on separate analyses of all vertebrate TM4SF protein (data not shown), TM4SF1, 4 and 18 form a monophyletic group and likely share a common ancestor. Hence, TM4SF1 and TM4SF18 are the most related in the TM4SF family. (C) Synteny analysis of vertebrate *Tm4SF1/4/18* in the human, mouse, chick, turtle and zebrafish genome assemblies. Dashed lines represent breaks in synteny. *TM4SF1, 4* and *18* are closely located on the same chromosome, suggesting that they were generated by two tandem gene duplications at early stages of vertebrate evolution. The first of these gave rise to the *TM4SF4* and *TM4SF1/18* paralogous groups, and the second gave rise to the *TM4SF1* and *TM4SF18* paralogous groups. The *tm4sf1* subfamily appears to have subsequently been lost in the lineage leading to teleost fish. Similarly, the *Tm4sf18* subfamily appears to have subsequently been lost in mice. (D) Percentage BLAST sequence identity (black numbers) and sequence similarity (red numbers) between teleost fish (zebrafish, medaka, tetraodon and fugu) Tm4sf18 and human, mouse or chick TM4SF1/18. Following the loss of tm4sf1, the remaining Tm4sf18 in teleost fish consistently shares higher protein sequence identity/similarity with human and chicken TM4SF1 over TM4SF18. Hence, zebrafish Tm4sf18 appears to have acquired the function of Tm4sf1 and is the predominant teleost homologue of mammalian TM4SF1.

Figure S3

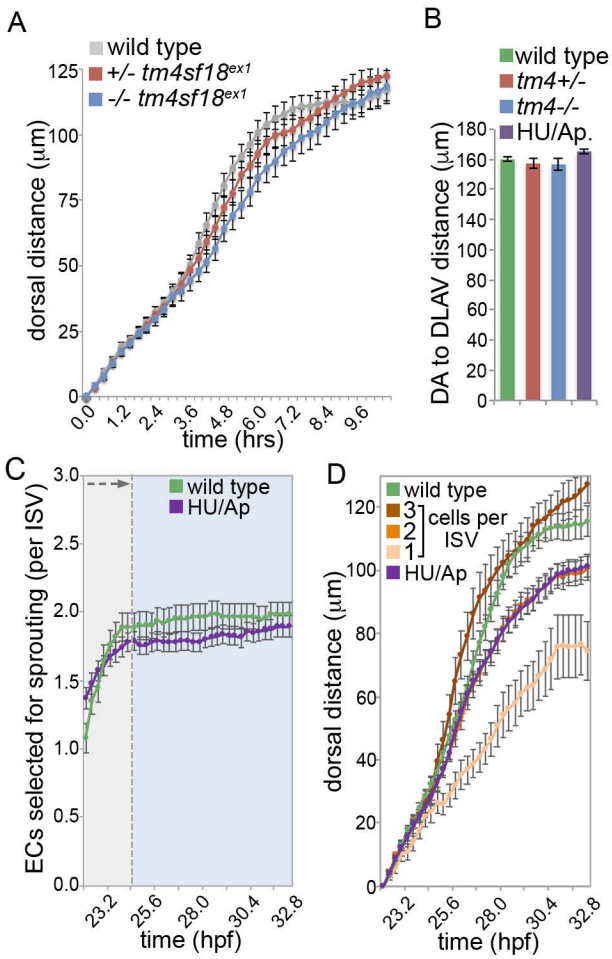

Figure S3. Phenotypic consequences of *tm4sf18* mutation and disruption of EC proliferation, related to Figure 3. (A) Quantification of the dorsal movement of tip ECs in wild type, *tm4sf18+/-* exon1 heterozygous mutant and *tm4sf18-/-* exon-1 homozygous mutant embryos. Mutation of only the long isoform of *tm4sf18* does not disrupt EC motility. (B) Quantification of the length of any fully formed ISVs observed in wild type, *tm4sf18+/-* heterozygous mutant, *tm4sf18-/-* homozygous mutant and hydroxyurea / aphidocolin (HU/Ap)-treated embryos. None of these perturbations affects the morphology of successfully formed ISVs. (C) Quantification of the number of ECs selected to branch into ISVs in wild type or HU/Ap-treated embryos. Disruption of EC proliferation has no significant effect on selection of motile ECs by lateral inhibition. (D) Quantification of the dorsal movement of tip ECs in ISV consisting of 1, 2 and 3 and more ECs and comparison with the motility of tip ECs in wild type and HU/Ap-treated embryos. Tip ECs in wild type embryos behave like those in ISVs with three cells whereas inhibition of proliferation generates tip ECs that behave like those in ISVs with only two cells, consistent with the average number of ECs per ISV in both of these situations (see Figure 3H). Error bars: mean ± SEM.